

Supporting Information

Energy Harvesting from Shadow-effect

*Qian Zhang^{a,1}, Qijie Liang^{b,1}, Sai Kishore Ravi^a, Dilip Krishna Nandakumar^a, Hao Qu^a, Lakshmi Suresh^a, Xueping Zhang^a, Yaoxin Zhang^a, Lin Yang^a, Andrew Thye Shen Wee^b, and Swee Ching Tan^a **

^a Department of Materials Science and Engineering, National University of Singapore, 9 Engineering Drive 1, Singapore 117574, Singapore.

^b Department of Physics, National University of Singapore, 2 Science Drive 3, Singapore 117551, Singapore.

* Corresponding author. e-mail: msetansc@nus.edu.sg

¹ These authors contributed equally to this work.

The SEM and AFM images of the SEG cell

The 3D image of the SEG cell is shown in Fig. S1a. A 15 nm thickness of the Au film was observed in Fig. S1b, which is a cross-view SEM of the SEG cell. The top-view SEM of the SEG cell is also shown in Fig. S1c. To observe the surface morphology clearly, the root-mean-square roughness values measured with AFM have been determined by the nanoscope software. Fig. S1d shows a fine grained structure in the Au film deposition on Silicon wafer.

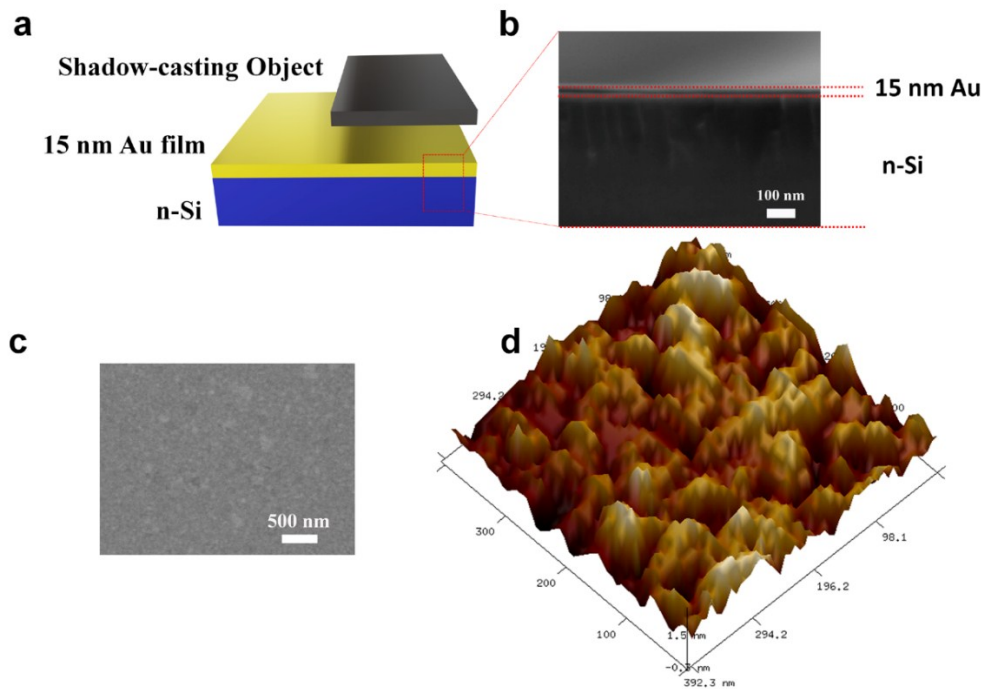


Fig. S1 (a) 3D image of the SEG cell. SEM image in (b) cross view and (c) top view of the SEG cell. (d) AFM image of top view of the SEG cell.

Comparison of cost between SEG and commercial silicon solar cells

SEG cell is composed of 15 nm Au film and n-Si. The cost of production of SEG cell of a size 1 m² is estimated, and tabulated in Table S2. Our analysis indicates the costs to be around 31.60 to 51.67 US dollars while the commercial solar panel is priced at 486.76 to 676.47 US dollar per square meter. The existing processes for commercial Silicon solar cell (C-Si cell) production includes high temperature and hazardous chemicals, but our SEG are less hazardous, safe and very easy to fabricate.

Table S1 Cost comparison of the SEG and C-Si cells

	Content/Brand		Cost (US\$ m ⁻²)
	SEG	n-Si (US\$ m ⁻²)	Coating 15nm Au film (Gold price 43.3 US\$ g ⁻¹)
19.10 (PVinsights)		12.50	31.60
39.17 (Sunpower)		12.50	51.67
C-Si	Atiter		486.76
	Sunpower		676.47

Performance of the bent SEG with 4 cells in parallel

The electrical output of the SEG with 4 Au/n-Si cells was investigated after it was bent under 1 sun intensity (1 kW m⁻²). The peak value of the short-circuit current (I_{sc}) and open-circuit voltage (V_{oc}) of the unbent SEG (180°) connected in parallel was up to 1.2 mA and 500 mV, respectively (Fig. S2a and Fig. S2b). With the bending angle varying from 30° to 240°, the I_{sc} and V_{oc} increases initially and then decreases, achieving the maximum value at 180° (Fig. S2c). The change in output is attributed to decrease in the illumination intensity in case of bent SEG.

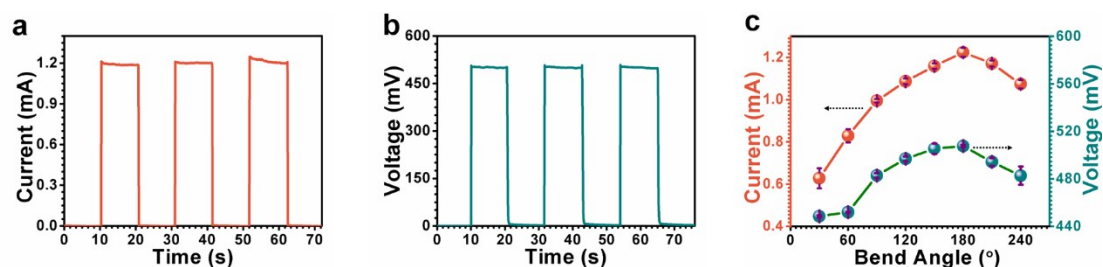


Fig. S2 Performance of the bent SEG with 4 cells in parallel. (a) The I_{sc} and (b) V_{oc} generated by the straight 4 SEG cells in parallel (180°). (c) electric performance changes of 4 SEG cells in parallel with different bending angles.

Photovoltaic properties of C-Si cell under different illumination intensity

The measured current density-voltage characteristics of C-Si cell below 1 sun, 0.8 sun, 0.2 sun and 0.1 sun intensity have been investigated. As shown in Fig. S3 and Table S1, the j_{sc} , V_{oc} and η (efficiency) of the C-Si decrease significantly towards lower light

intensity. FF in Table S1 is fill factor of the C-Si cell.

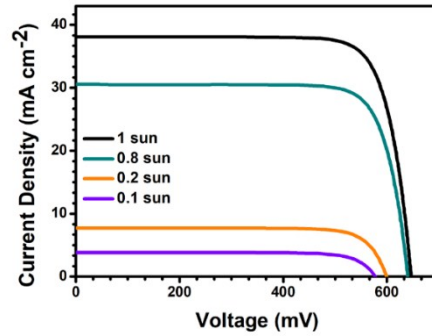


Fig. S3 Current density-voltage curves of C-Si cell at different light intensity.

Table S2 Photovoltaic Properties of C-Si cell at different light intensity

	j_{sc} (mA cm ⁻²)	V_{oc} (mV)	η (%)	FF
1 sun	38.10	647	19.59	0.795
0.8 sun	30.52	640	19.48	0.798
0.2 sun	7.70	599	18.45	0.799
0.1 sun	3.82	577	17.51	0.794

Electrical performance of SEG cell under fully illumination at various incidence angles

The incidence angle was changed by parallel moving SEG cells to different relative positions with light source. As shown in Fig. S4, the angle when the SEG cell in middle position was set to be 0°. In this case, the I_{sc} and V_{oc} generated by SEG cell is 1.2 μ A 15 mV, respectively. There could be some inherent work-function non-uniformity on the metal-coated Si; this could be due to a non-uniformity in the coating itself; surface impurities sharply alter the work function as well, so any slight gradient in work function (not necessarily light-induced) could drive this current. When the SEG cell was parallel moved to left position, the angle changed to be α while moved to right position is β . When α is 60°, the I_{sc} and V_{oc} all increased. In addition, the I_{sc} and V_{oc} changed to be negative when the SEG in right position ($\beta = -60^\circ$). As long as the sample is not very small that it falls within an area of uniform light intensity under a perfectly parallel beam (or unless we use some dedicated optics to ensure a parallel beam of light throughout sample area), an intensity gradient is unavoidable that could result in a

minor work function gradient driving this small photocurrent.

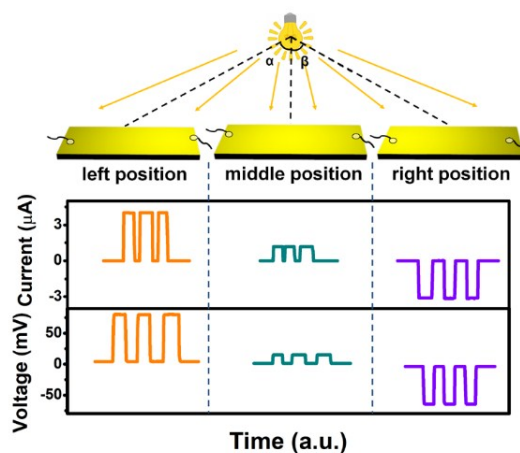


Fig. S4 Electrical performance of SEG cell at various incidence angles.

The front view photograph of SEG cell and a test circuit diagram

The front view photograph of SEG cell is shown in Fig. S5. The red electrode is connected with the in-shadow part of SEG cell while the black electrode is connected with the illuminated part of SEG cell. In otherwise, an insulating glass is attached on the back side of the SEG cell to prevent the electrodes connecting with the silicon film of the SEG cell. The Keithley K2400 was used as a characterize meter and connected in the circuit.

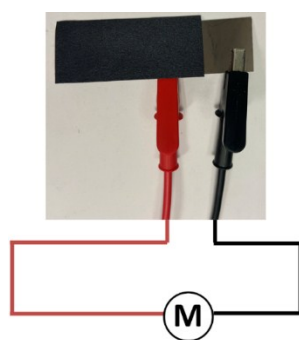


Fig. S5 Front view photograph of one SEG cell and circuit diagram for measurement.

The KPFM image of SEG cell

Surface potential of SEG cell (15 nm Au film) in shadow is shown in Fig. S6a while under complete illumination is shown in Fig. S6b. The average surface potential is about 4.94 eV and 5.07 eV, respectively.

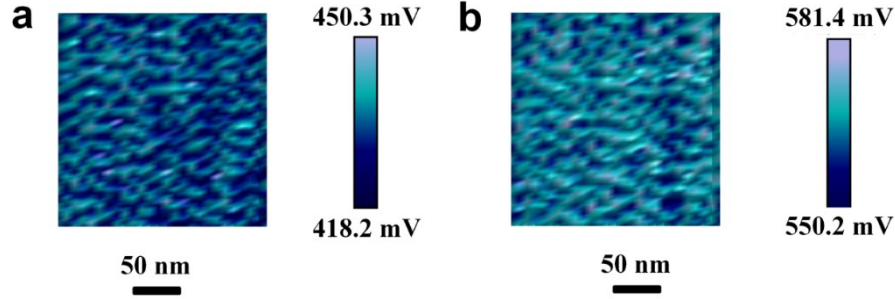


Fig. S6 Surface potential maps of SEG cell (15 nm Au film) before (a) and after (b) full illumination.

Current-Voltage (I-V) characteristics of Au film half on n-Si and Si

The I-V characteristics of the 15 nm Au film half on n-Si and n-Si were detected in shadow or under illumination, respectively. As shown in Fig. S7, under illumination, the resistance of the Au film half on n-Si was lower than Au/n-Si in shadow. The resistance of n-Si (irrespective of being illuminated or in shadowed) is much larger than Au film half on n-Si (under illumination).

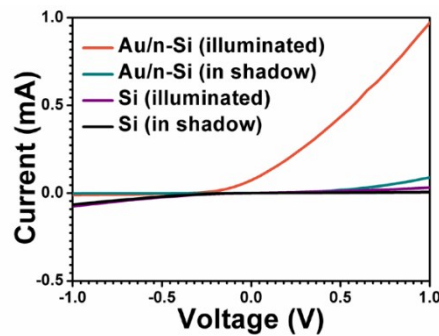


Fig. S7 I-V curves of Au film half on n-Si and n-Si in shadow or illuminated.

Details of performance characterization of SEG cells

As shown in Fig. S9a, the I_{sc} generated by SEG cells with 30nm, 60 nm, 120 nm and 240 nm Au film are 98 μ A, 17 μ A, 2 μ A and 1 μ A, respectively. In Fig. S9b, the V_{oc} generated by SEG cells with 30nm, 60 nm, 120 nm and 240 nm Au film are 42 mV, 10

mV, 0.57 mV and 0.03 mV, respectively. The I_{sc} and V_{oc} generated by the SEG cell with 15 nm Au film exhibit the highest responses as compared to those generated by the SEG cells with 30nm, 60 nm, 120 nm and 240 nm Au film.

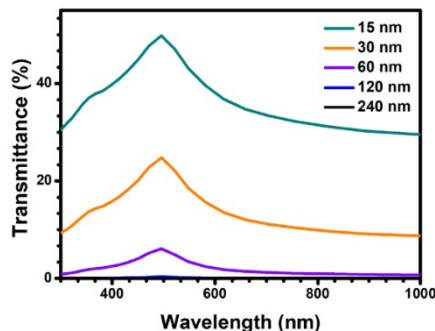


Fig. S8 Details of performance characterization of SEG cells. (a) I_{sc} and (b) V_{oc} generated by SEG cell with 15 nm, 30nm, 60 nm, 120nm, 240 nm Au film.

The Au film was coated on transparent glass by thermal evaporator, which is the same as Au film coating on the silicon wafer. The transmittance of the Au films with 15 nm, 30 nm, 60 nm, 120 nm, 240 nm are shown in Fig. S8.

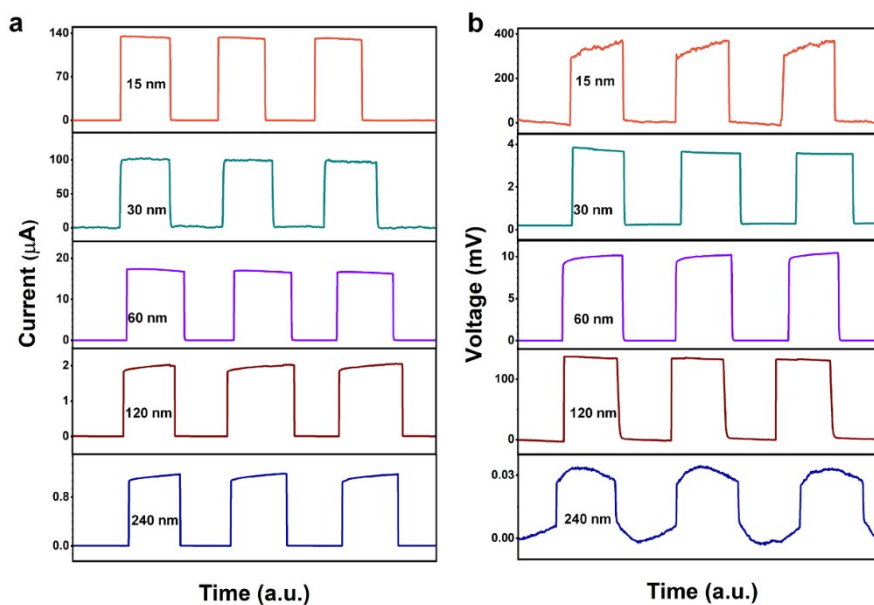


Fig. S9 Transmittance of the Au film with different thicknesses.

Size and area effect

The effect of sample size was studied under two conditions:

1. Fixed width of 2 cm and increasing length of the sample.
2. Fixed length and increase the width of the sample.

In all these cases, the samples were kept half-in-shadow and the connection point was the midpoint of the illuminated and dark surfaces. Fig. S10 shows the performance of the device under different conditions. The power density (P_{hi}) is calculated from Equation (1). The performance of the device depends on two factors - electron generation and electron transport to the dark side from where it can be collected. The electron generation is mainly influenced by the surface area of illumination, since more the area of illumination, more will be the amount of excited electrons. The transport of the excited electrons is primarily affected by the electric field that is formed at the interface. This field decreases as the distance of the collection point from the interface increases.

With the sample width fixed, there is an increase in the performance of the device as the sample size increases because of the increase in surface area of illumination with increasing sample size. This translates into more excited electrons and hence more current. On the other hand, the voltage is influenced only by the intensity of the illuminated light. Hence, it remains constant. The minor variation may be attributed to non-uniformities in the Au coating on the n-Si and some surface impurities.

In case of the sample length being fixed, a width of 2 cm gives the maximum output because it offers an optimum area of electron generation and electron collection. Larger samples might have a larger rate of electron generation, but the efficiency of collection is hampered because of the non-uniformity in the electric field that drives the electrons towards the dark side. In case of smaller samples, the rate of electron generation is less owing to lesser surface area under illumination.

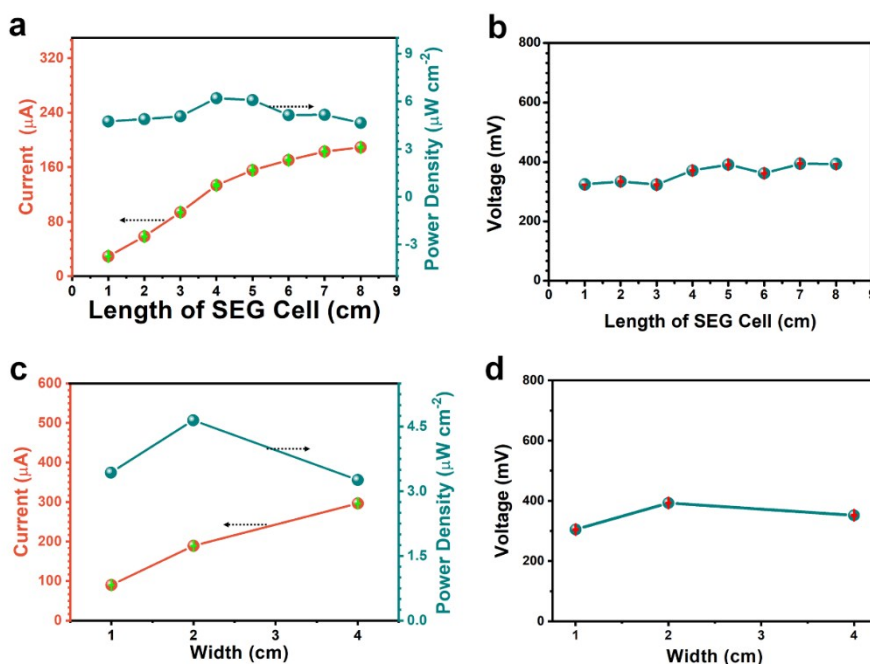


Fig. S10 (a) I_{sc} , power density and (b) V_{oc} of SEG cell with fixing the width to be 2 cm and changing the length of the SEG cell from 8 cm to 1 cm. (c) I_{sc} , power density and (d) V_{oc} of SEG cell with fixing the length to be 8 cm and changing the length of the SEG cell from 4 cm, 2 cm to 1 cm.

Details of performance characterization of SEG cells with 15 nm Cu film and 15 nm Al film

In Fig. S11, the I_{sc} and V_{oc} generated by the SEG cell with 15 nm Al film are all lower than that of SEG cells with 15 nm Au film and 15 nm Cu film. The I_{sc} generated by SEG cell with 15 nm Al film is 0.23 μA . The I_{sc} and V_{oc} of the SEG cell with 15 nm Cu film decreased gradually with three cycles of light ON and OFF.

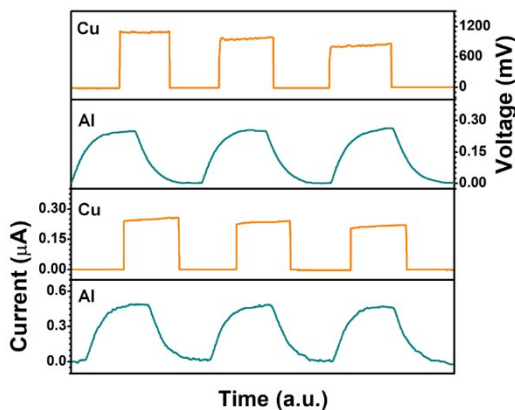


Fig. S11 V_{oc} and I_{sc} generated by SEG cells with 15 nm Cu film and 15 nm Al film.

Surface potential map and work function shift of SEG cell with 15 nm Cu film and 15 nm Al film

The surface potential map of SEG cell with 15 nm Cu film and 15 nm Al film was measured using KPFM. As shown in Fig. S12, the shift in work function of the SEG cell with 15 nm Cu film under illumination and in dark is calculated to be about 0.11 eV while the SEG cell with 15 nm Al film is 0.03 eV.

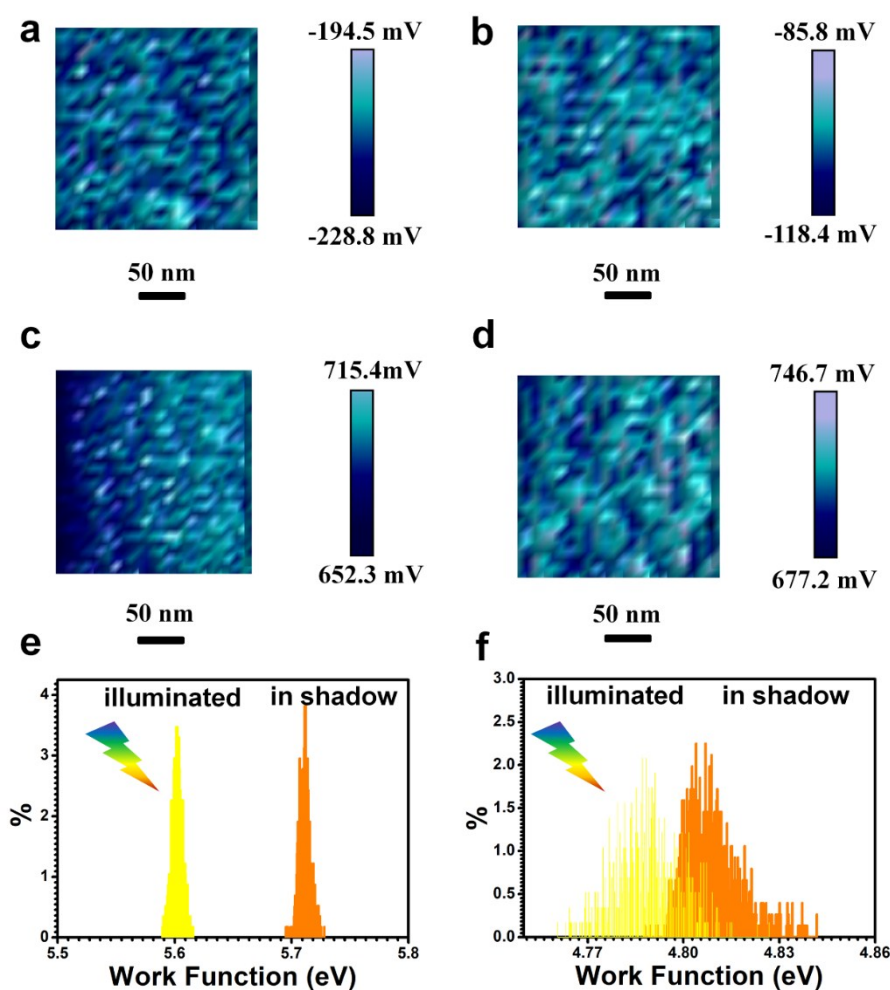


Fig. S12 Surface potential maps of SEG cell with 15 nm Cu film before (a) and after (b) full illumination. Surface potential maps of SEG cell with 15 nm Al film before (c) and after (d) full illumination. Work function shift of (e) SEG cell with 15 nm Cu film and (f) SEG cell with 15 nm Al film under illuminated or in shadow.

Performance characterization of SEG cells with planar n-Si and textured n-Si

Comparing with a planar n-Si, the surface modification of the silicon increases surface area and reduces reflection of incident light. As shown in Fig. S13, the I_{sc} of SEG cell with textured n-Si has a photocurrent response of 343 μA is larger than that obtained with planar n-Si which only has a photocurrent response of 134 μA . However, the V_{oc} of SEG cell with textured n-Si is 371 mV is smaller than that obtained with planar n-Si (78 mV). This is probably attributed to the facet that each side of the pyramid of textured n-Si experiencing different light intensity while the light illumination on uniform film of planar n-Si is very uniform which results in uniform work function shifts.

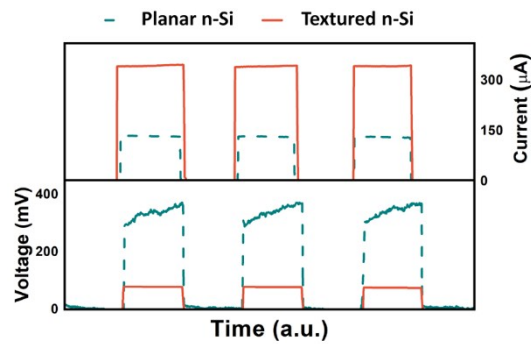


Fig. S13 Performance characterization of SEG cells with planar n-Si and textured n-Si

Photographs taken from the side of SEG cell

Fig. S14a is the photograph of the individual SEG cell as a number counter sensor for robot taken from the side of SEG cell. Fig. S14b is the photograph of the SEG cell as a position detector for remote-controlled car. As shown in these photographs, half of the SEG cells were covered.

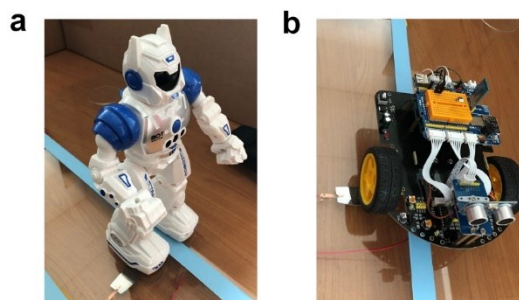


Fig. S14 Photographs taken from the side of SEG cell. (a) Photograph of the SEG cell as a number counter sensor for robot, and (b) Photograph of the SEG cell as a position detector for remote-

controlled car, which are all taken from the side of SEG cell.

Circuit diagram of the electronic interface

To fabricate a sensor system to record the number of times the robot pass by, a SEG cell was used as a sensor and connected to the electronic interface as shown in the circuit diagram in Figure S15a1. The SEG cell represented by S is connected with Arduino NANO pin A1. Also, an 1 M Ω resistor is connected with A1 to make it ground (to keep the reading is 0 V) when there is no voltage generated by SEG cell. Arduino NANO microcontroller is used to measure the DC voltage output from the SEG cell. The LCD screen relates to Arduino NANO via LCD i2c. Pin 17,18,19,20 on LCD i2c are connected to Arduino NANO gnd, A5, A4, 5V. The LCD screen is able to display 26 English alphabets and numbers as the library is pre-loaded into the Arduino NANO. The sensor system is programmed to read the voltage from SEG cell continuously. When there is a robot passing by the SEG cell, it will generate a voltage. Thus the Arduino NANO could measure the total voltage and send the number to LCD Screen. The element diagram is also shown in Fig. S15a2.

The sensor system to detect track of the remote-controlled car was also fabricated. As shown in Fig. S15b1, the SEG cells are represented as S1, S2 which are connected with Arduino UNO pin A1 and A2. Also, two 1 M Ω resistors are connected with pin A1 and pin A2 to ground to make sure the low level of voltage when generator is inactive. There are two LED lights on Arduino pin D8, pin D9. The Arduino UNO will take voltage reading from SEG cells, every 50 ms. Initially two LEDs are off. When the remote-controlled car passed through the SEG cell S1, the LED on pin D8 was turned on by Arduino UNO to show that remote-controlled car was on position 1 where the SEG cell S1 was. When the car passed through the SEG cell S2, the LED on the pin D9 was turned on by Arduino UNO to show that remote-controlled car was on position 2 where the SEG cell S2 was. The element diagram is also shown as Fig. S15b2.

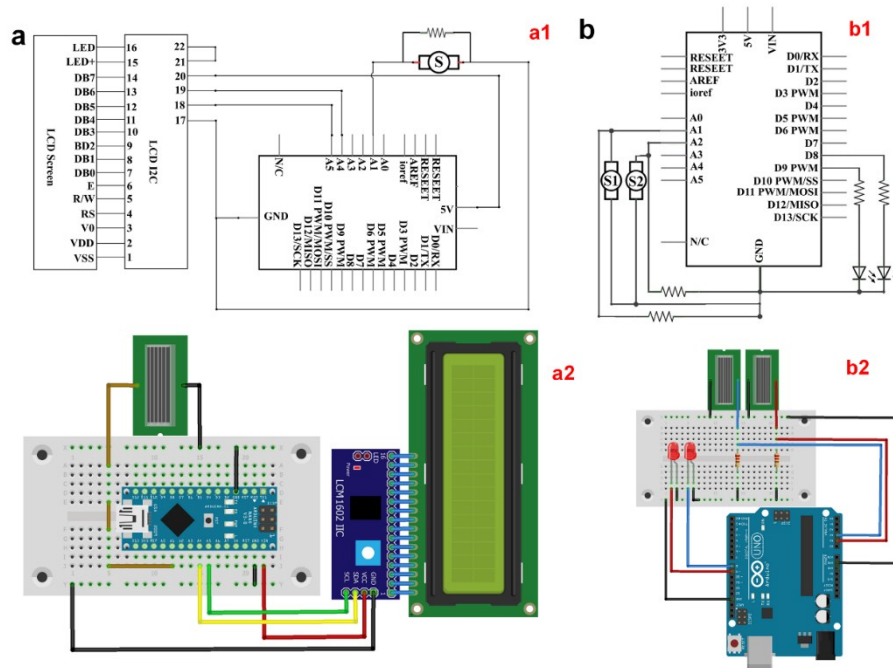


Fig. S15 Circuit diagram of the electronic interface. (a) Circuit diagram (a1) and element diagram (a2) of sensor system to record the number of times the robot pass by. (b) Circuit diagram (b1) and element diagram (b2) of sensor system to detect track of the remote-controlled car.

Stability of the SEG as a self-powered sensor

The stability of the SEG as a self-powered sensor was examined through continuously stepping on top of the SEG in glass frame (0.844 sun) for over 1000 cycles, as exhibited in Fig. S16. The voltage response was measured after every 250 cycles, during which 70 cycles were recorded and also displayed. The voltage only shows a deviation rate about 3.9% through 1000 cycles, which the stability of the SEG as a sensor is confirmed.

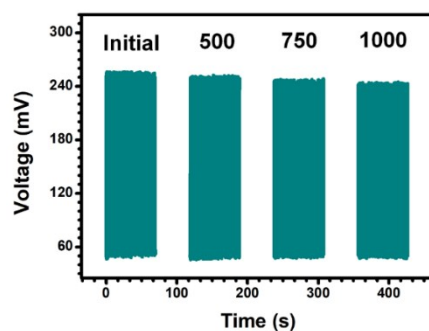
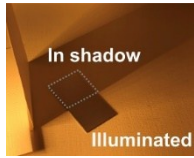
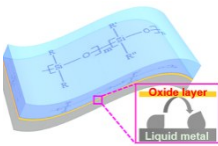
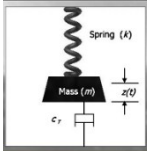


Fig. S16 The stability test for the SEG as a self-powered sensor with continuous stepping on top of the SEG in glass frame (0.844 sun) for 1000 cycles.

Advantages of SEG by comparing with other energy harvesting devices

Table S3 is the comparison between different types of energy harvest technologies which ranging from a few milli-watt to few micro-watt. Contrary to the other energy harvest technologies, which requires complex design intricate engineering and expensive raw materials, the fabrication of the SEG can be done at extremely low cost and does not involve any harmful chemicals nor intricate synthesis protocols. The SEG have twice the efficiency of commercial solar cell in a weak ambient light. These advantages make the SEG an attractive device for many applications.

Table S3 Key characteristics of different kinds of energy harvester

	SEG ^[this work] 	Commercial solar cell ^[this work] 	Triboelectric nanogenerator ^[s1] 	Micro-electromagnetic generator ^[s2] 
Structure	Metal thin film-semiconductor	Formed from multiple crystals of silicon	Galinstan-silicone rubber	Spring-mass-damper system
Energy conversion type	Low intensity light energy	Light energy	Mechanical energy	Vibration energy
Power density	0.14 $\mu\text{W cm}^{-2}$ (0.001 sun, half-in-shadow)	0.07 $\mu\text{W cm}^{-2}$ (0.001 sun, half-in-shadow)	8.43 mW m^{-2}	307 $\mu\text{W m}^{-3}$
Application	self-powered proximity sensor to detect movement of objects	Light energy harvester	Mechanical energy harvester	Vibration energy harvester
	Weak ambient light energy harvester			Potential application as wireless sensor node

References

s1. Yang, Y., Sun, N., et al. Liquid-Metal-Based Super-Stretchable and Structure-Designable Triboelectric Nanogenerator for Wearable Electronics. *ACS Nano*, **12**, 2027-2034 (2018).
s2. Beeby, S. P., Torah, R. N., et al. A micro electromagnetic generator for vibration energy harvesting. *Journal of Micromechanics and Microengineering*, **17**, 1257-1265 (2007).